ELSEVIER

Journal of Molecular Catalysis A: Chemical 112 (1996) 235–251

JOURNAL OF MOLECULAR CATALYSIS A: CHEMICAL

# Ethoxylation of fatty alcohols promoted by an aluminum alkoxide sulphate catalyst

M. Di Serio [a], P. Iengo [a], R. Gobetto [b], S. Bruni [c], E. Santacesaria [a,*]

[a] *Dipartimento di Chimica dell' Università di Napoli "Federico II", Via Mezzocannone 4, 80134 Napoli, Italy*

[b] *Dipartimento di Chimica Inorganica, Chimica Fisica e Chimica dei Materiali, Università di Torino, Via Pietro Giuria 7, 10125 Torino, Italy*

[c] *Dipartimento di Chimica Inorganica, Metallorganica e Analitica, Università di Milano, Via Venezian 21 - 20133 Milano, Italy*

Received 27 November 1995; accepted 4 April 1996

**Abstract**

Aluminum alkoxides are moderately active in promoting the ethoxylation of fatty alcohols. When these alkoxides are treated with pure sulfuric acid (100% by weight) in a stoichiometric ratio, the catalytic activity is strongly increased initially but it decreases rapidly giving place to products being very interesting for industry as they contain not more than two or three ethylene oxide adducts. These products are useful as raw materials for producing surfactants by sulphonation. Aluminum in the catalyst used shows all the possible coordination numbers, as demonstrated with the aid of $^{27}Al$ NMR. The catalyst shows a very feeble Bronsted activity. As a consequence, small amounts of polyglycols are formed during reaction, in respect to the large amounts of ethoxylated dodecanol. Reaction rates are strongly inhibited by the presence of a Lewis base such as, for example, triphenylphosphine. The reaction seems to occur in the coordination sphere of the aluminum atoms. Other factors influencing activity and selectivity have been examined and a kinetic model has been developed on the basis of a reasonable reaction mechanism.

*Keywords:* Ethoxylation; Fatty alcohols; Aluminium catalysts

## 1. Introduction

A great number of patents has recently been published dealing with catalytic systems promoting narrow-range ethoxylation (NRE), i.e. ethoxylation of fatty alcohols with a narrow distribution of the molecular weights of the ethoxylated oligomers and containing a very low concentration of the residual unreacted alcohol. Products of this type have better properties than those produced with the traditional alkaline catalyst KOH and for low ethylene oxide/substrate molar ratio, can be sulphonated without forming undesired dioxane [1]. Despite the large interest shown by the industry in these products, very few scientific papers have been published devoted to the behavior and structure of the catalysts able to promote NRE, to the possible reaction mechanisms giving narrow distributions, and to the comparison of the behavior of these catalysts with that of the most used and traditional catalyst KOH. The behavior of the traditional catalyst KOH has been studied

* Corresponding author. Tel.: +39-81-5476544; fax: +39-81-5527771.


*PII* S1381-1169(96)00134-3

by Santacesaria et al. [2–5] and still by Santacesaria et al. [6] it has been compared with that of an alkaline earth catalyst, that is, the first discovered NRE catalytic system (see for example Refs. [7,8]). Alkaline earth catalysts promote NRE because they affect proton transfer equilibria, as demonstrated by Santacesaria et al. [6].

Very efficient NRE catalysts are some Lewis acids (see for example Ref. [9]). In particular, two patents [10,11] have recently proposed the use of an aluminum alkoxide treated with concentrated sulfuric acid as a possible NRE catalyst of high efficiency.

We studied this catalytic system for what concerns: the structure of the catalyst, its kinetic behavior and the reaction mechanism originating the narrow distribution of the oligomers. This catalyst has a peculiar kinetic behavior if compared with that of the traditional catalyst KOH. The reaction starts with a very high rate, but, after the addition of about one mole of ethylene oxide per mole of the substrate, the activity of the catalyst strongly decreases. As a consequence, fatty alcohol is quickly consumed and the distribution of the oligomer can be limited to the addition of a small number of ethylene oxide adducts. Therefore, narrow range distribution is essentially originated from the strong difference among the initiation and the propagation constants, that is $k_i \gg k_p$. The reasons for this behavior will be examined and discussed. Finally, on the basis of the experimental observations, a reaction mechanism will be proposed and a kinetic model, able to simulate the kinetic runs performed, will be developed.

## 2. Experimental

### 2.1. Apparatus, methods and reagents

#### 2.1.1. Preparation of the catalyst and techniques used for characterization

The catalyst has been prepared by reacting, first of all, aluminum isopropoxide with 1-dodecanol in a stoichiometric amount. The following exchange reaction occurs:

$$Al(i-PrO)_3 + 3ROH \rightarrow Al(OR)_3 + 3i-PrOH \quad (1)$$

The reaction is performed at about 130°C. At this temperature the formed isopropanol is easily stripped with a nitrogen stream and collected in a cooled graduated cylinder. The aluminum tridodecanoxide formed is liquid at reaction temperature, but condenses below 50°C giving a white amorphous solid. $Al(i\text{-}PrO)_3$ is almost completely converted as it resulted from the collected amount of isopropanol. After the exchange reaction (1) temperature was lowered at 50°C and then sulfuric acid (100%) was added dropwise to the aluminum tridodecanoxide, under vigorous stirring of the solution, until reaching a prefixed molar ratio $H_2SO_4/Al$ between 0 and 1. The reaction occurring in this case is:

$$Al(OR)_3 + H_2SO_4 \rightarrow Al(OR)SO_4 + 2ROH \quad (2)$$

We attempted without success to remove free dodecanol by heating the reaction mixture under vacuum. This fact indicates that dodecanol is probably strongly bounded to aluminum atoms in the way shown in Scheme 1 and it may be responsible for the weak Bronsted acidity observed. This type of acidity has been evidenced according to the way suggested by Benesi [12] and corresponds to the color change of methyl yellow occurring at $pK_a = 3.3$.

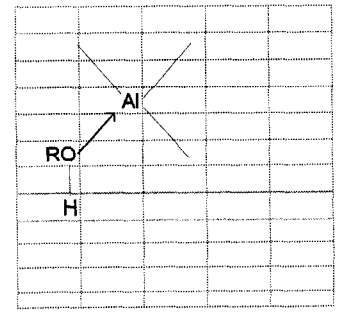


(3)

Scheme 1.

The addition of sulfuric acid to aluminum tridodecanoxide determines a strong increase of the viscosity of the solution. This fact suggests the occurrence of molecular condensation with an increase in the molecular weight of the aluminum complexes. The catalyst so prepared was then submitted to the IR and $^{27}Al$ NMR analysis. The IR spectra were recorded in the region from 4000 to 400 $cm^{-1}$ by means of a Digilab FTS-40 spectrophotometer. The spectrum of aluminium tridodecanoxide was obtained on a KBr pellet of the compound, while the spectra of 1-dodecanol and aluminum tridodecanoxide treated with sulfuric acid were observed by placing a small amount of each substance between two pellets of pure KBr. To prevent hydrolysis of the aluminum compounds, the samples were prepared in a glove bag under $N_2$ atmosphere and KBr was previously desiccated in an oven at 100°C. The IR spectrum of aluminium tridodecanoxide treated with sulfuric acid was recorded at 100 K in order to resolve the broad bands observed at room temperature in the frequency region of sulphate vibrations.

$^{27}Al$ NMR spectra were obtained on a JEOL EX400 spectrometer operating at 104.16 MHz. Chemical shifts are reported downfield positive in respect to $[Al(H_2O)_6]^{3+}$. The spectra were acquired with 90° pulse of 12.5 ms, recycle delay of 0.185 s and a number of transient of 5000–10000.

### 2.1.2. *Ethoxylation reactor, operative conditions, analysis and reagents*

Kinetic runs were performed in a 1.5 L jacketed stainless steel reactor equipped with a magnetically driven stirrer, consisting in a turbine connected as in Fig. 1 to a holed rod able to develop a great interfacial area. The reactor was supplied by Inox Impianti. The control of pressure, temperature and ethylene oxide feeding the reactor was fully automatized by a computer. The ethylene oxide consumption was directly measured and recorded at each instant with a weight balance connected to the computer measuring the weight loss of the ethylene

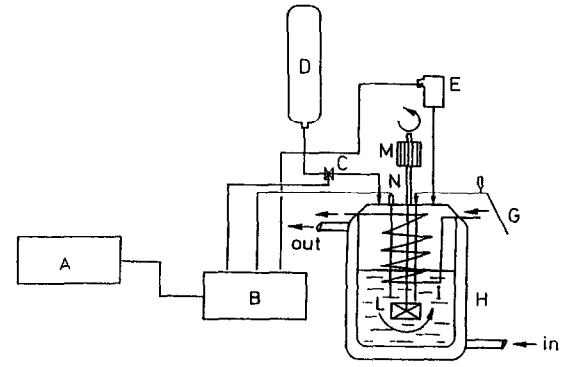


Fig. 1. Scheme of the automated plant employed in ethoxylation. A = computer; B = computer interface; C = on–off valve for feeding ethylene oxide; D = ethylene oxide bottle; E = pressure transducer; G = exit for withdrawing; H = jacketed reactor; I = freezing coil; L = holed stirrer; M = magnedrive stirrer; N = thermocouple.

oxide bottle. The ethylene oxide bottle was pressurized with nitrogen at about 10 atm.

Temperature and pressure were controlled and recorded at each instant. Temperature was kept constant by using two thermostated fluids, one for heating and the other for freezing the reaction mixture. The heating fluid circulated in the reactor jacket, the freezing one was fed, when necessary, in a coil inside the reactor. Ethylene oxide was automatically fed to the reactor to keep a preset pressure value constant.

Kinetic runs were performed at different temperatures, pressures, catalyst concentrations and $H_2SO_4/Al$ molar ratio. Temperatures were changed in the range 100–150°C, pressure in the range 1–2 atm, catalyst concentrations in the range 0.6–1.5% in moles of aluminum, and the molar ratio $H_2SO_4/Al$ from 0 to 1.

Samples of the reaction mixtures were taken from the reactor at different times and chromatographically analyzed by HPLC, after derivatization with 3,5-dinitrobenzoylchloride, following the method suggested by Desberre et al. [13]. The HPLC column used was a 25 cm long Lichrospher 100 Diol with 0.4 cm diameter, supplied by Merck. The elution gradient technique was employed with a solvent A [99/1 (v/v) = *n*-eptane/$CH_2Cl_2$-2-propanol (95/5)] and a solvent B [ 60/40 (v/v) = *n*-

Table 1
Elution gradient program in the HPLC analysis of ethoxylated oligomers

| T (min.) | A (vol%) | B (vol%) |
|---|---|---|
| 0 | 100 | 0 |
| 80 | 0 | 100 |
| 90 | 0 | 100 |
| 110 | 100 | 0 |

eptane/$CH_2Cl_2$-2-propanol (95/5)]. The elution gradient program is reported in Table 1. The solvent feed rate was 0.0166 $cm^3/s$ and the UV detector was kept at 254 nm. The response of the detector was the same for all the oligomers.

In order to interpret kinetic data, the values of the densities of the reaction mixtures and solubilities of the ethylene oxide in those mixtures must be known. Densities can be calculated with the empirical relation:

$$d = 0.86 + 2.5 \cdot 10^{-2} n_{EO} - 4.76 \cdot 10^{-4} n_{EO}^2 - 2.69 \cdot 10^{-5} n_{EO}^3 - 7.7 \cdot 10^{-4} T \quad (3)$$

determined by regression on many experimental data by Di Serio et al. [5], $n_{EO}$ is the mean number of ethylene oxide adducts.

Solubilities were calculated as suggested by Di Serio et al. [5] according to the Wilson equation using the following parameters:

$$\Lambda_{12} = 13.00 + 0.9611 n_{EO} - 1.967 \cdot 10^{-2} n_{EO}^2 \quad (4a)$$

$$\Lambda_{21} = -0.4069 + 4.714 \cdot 10^{-2} n_{EO} - 1.340 \cdot 10^{-3} n_{EO}^2 \quad (4b)$$

All the reagents were supplied by Aldrich at the highest degree of purity available. Ethylene oxide was supplied by SIAD.

## 3. Results and discussion

### 3.1. IR catalyst characterization

IR spectra have been recorded for comparison purposes respectively on 1-dodecanol, aluminum tridodecanoxide and aluminium tridodecanoxide treated with sulfuric acid in the molar ratio 1:1.

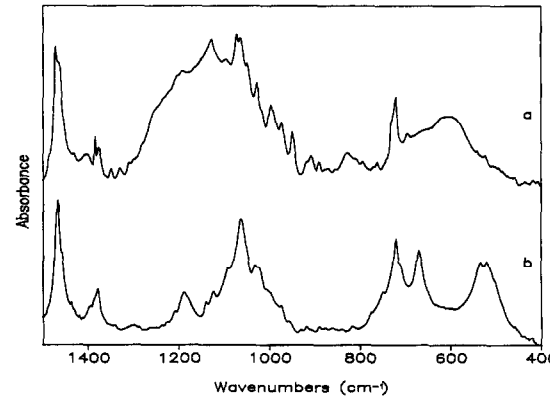


Fig. 2. IR spectra (1500–400 $cm^{-1}$) of: (a) aluminium tridodecanoxide treated with $H_2SO_4$ (molar ratio 1:1) and (b) aluminium tridodecanoxide untreated (KBr pellet). Spectrum (a) was obtained at 100 K and spectrum (b) at room temperature.

The spectrum of aluminium tridodecanoxide (Fig. 2b and Table 2) shows, besides bands that, being observed also for the corresponding alcohol, can be assigned to vibrational modes of the paraffinic chain [14], two bands at 1063 and 1031 $cm^{-1}$ and three bands at 670, 533 and 519 $cm^{-1}$ that are absent in the spectrum of 1-

Table 2
IR vibrational frequencies ($cm^{-1}$), in the region 1500–400 $cm^{-1}$, of aluminium tridodecanoxide untreated and treated with sulfuric acid in molar ratio 1:1

| Compounds | | Assignment |
|---|---|---|
| $Al(OR)_3$ | $Al(OR)_3 + H_2SO_4$ 1:1 | |
| 1468s | 1471s | scissoring $CH_2$ |
| 1460sh | 1464sh | $\delta_{as}(CH_3)$ |
| 1379m | 1377m | $\delta_s(CH_3)$ |
| | 1192sh | |
| | 1127s | $\nu_3(SO_4^{2-})$ |
| | 1072s | |
| 1063s | 1064s | $\nu$(C–O) |
| 1031m | 1028m | $\nu$(C–O) |
| | 997m | $\nu_1(SO_4^{2-})$ |
| 721ms | 721m | rocking $CH_2$ |
| | 696sh | $\nu_4(SO_4^{2-})$ |
| | 615–602b | |
| 669ms | | $\nu$(Al–O) |
| 532m | | $\nu$(Al–O) |
| 519m | | $\nu$(Al–O) |

s = strong, m = medium, sh = shoulder, b = broad.

dodecanol and can be attributed respectively to C–O and Al–O stretching modes. The suggested assignments are consistent with those proposed by Barraclough et al. [15] to interpret the vibrational spectra of some metal alkoxides. It is worth noting that, according to these authors, the band at about 1060 $cm^{-1}$ should be assigned to terminal alkoxide groups, while the one at about 1030 $cm^{-1}$ to bridging alkoxide groups, thus indicating an oligomeric structure of the examined compounds. This might also be the case for aluminum tridodecanoxide, even if the number of bands observed for metal–oxygen vibrations is not in contradiction with the hypothesis of a monomeric structure.

In order to obtain structural information from the IR spectrum of aluminium tridodecanoxide treated with sulfuric acid, it is useful to recall how the activity and number of the vibrational modes of $SO_4^{2-}$ change when the ion is coordinated to a metal atom [16]. Nakamoto [16] reported the possible structures of the metal complexes with sulfuric acid and the corresponding IR absorption bands, see Scheme 2. The free sulphate ion belongs to the $T_d$ point group and four fundamental vibrational modes are expected: $\nu_1$ ($A_1$), $\nu_2$ (E), $\nu_3$ ($T_2$) and $\nu_4$ ($T_2$), among which only $\nu_3$ and $\nu_4$ are infrared active, giving rise to bands at about 1100 and 600 $cm^{-1}$. In the unidentate coordination mode, the symmetry lowers to $C_{3v}$, causing the appearance in the IR spectrum of bands corresponding to $\nu_1$ and $\nu_2$, while the degeneracy of $\nu_3$ and $\nu_4$ is partially removed, each one giving rise to two bands. In the bidentate coordination

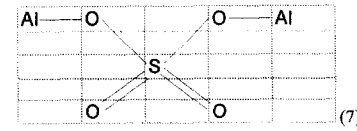

(7)

Scheme 3.

mode, both chelating and bridging, the symmetry of the sulphate becomes $C_{2v}$, that leads to the complete splitting of $\nu_3$ and $\nu_4$ into three bands (see also Ref. [17]). Bridging and chelating sulphate groups cannot therefore be distinguished on the basis of symmetry, but it has been observed that the sulphur–oxygen stretching frequencies are higher for the latter than for the former one: for example, Barraclough et al. [15] report bands at 1195, 1110, 1030 and 960 $cm^{-1}$ for $Pd(NH_3)_2SO_4$ (bridged) and at 1240, 1125, 1040–1015 and 955 $cm^{-1}$ for $[Pd(phen)SO_4]$ (chelated).

On the basis of the above considerations, in the spectrum of our catalyst (Fig. 2a and Table 2) we assign to a bridging bidentate coordinated sulphate group, of the type shown by Scheme 2, the bands at 1192, 1127 and 1072 $cm^{-1}$ ($\nu_3$) and the band at 997 $cm^{-1}$ ($\nu_1$). The bands at 696, 615 and 602 $cm^{-1}$ can be tentatively assigned to the $\nu_4$ mode of the same group, even if in this spectral range also bands due to Al–O stretching vibrations should be observed; finally, no band can be easily individuated between 500 and 400 $cm^{-1}$, where the $\nu_2$ frequency should fall.

The structure in Scheme 3 seems to be dominant and explains well the increase of the vis-

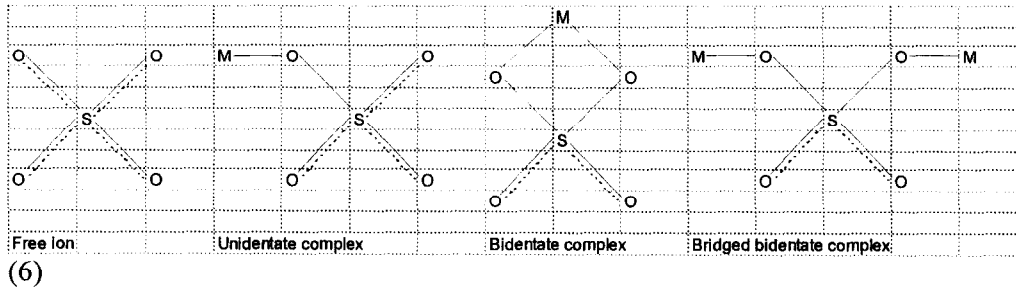

(6)

Scheme 2.

cosity of the product during the addition of sulfuric acid. Moreover, the bidentate structure in Scheme 3 should have Lewis superacidic properties in analogy with similar structures proposed by Hino and Arata [18] and Arata [19] for zirconium oxide treated on the surface with sulfuric acid, see Scheme 4. In a recent review Misono and Okuhara [20] considered the zirconium oxide, treated with sulfuric acid, at the top level as a solid Lewis superacid, but no information is available on sulphated aluminum.

Scheme 4, in the presence of water, shows Broensted acidity, too, as evidenced by the scheme reported above. Also, our catalyst exhibits low Broensted acidity, confirmed, as previously mentioned, by the behavior of some indicators with different $pK_a$ [12]. On the basis of the IR spectrum, this acidity can be attributed to the presence of metal coordinated alcohol, demonstrated by a broad absorption band with components at 3379, 3262, 3224 and 3144 $cm^{-1}$, assigned to O–H stretching modes and by a band at $\sim 1640$ $cm^{-1}$, assigned to the O–H bending mode of coordinated dodecanol [21]. By concluding, IR spectra suggest the formation of a bidentate structure of the type shown in Scheme 5, in which the strong inductive effect of the sulphate group favors the formation of very strong Lewis acid sites and weak Bronsted ones according to Scheme 5.

### 3.2. $^{27}Al$-NMR catalyst characterization

Spectra have been made for the original reagent aluminum isopropoxide, aluminum tridodecanoxide and aluminum tridodecanoxide treated with different amounts of sulfuric acid, corresponding to the molar ratios $H_2SO_4/Al$ 0.25, 0.5 and 1, respectively. These spectra obtained are reported in Fig. 3. Again, before interpreting them, we briefly summarize what is known from literature about this argument. According to Akitt [22] aluminum alkoxides can assume oligomeric structures such as shown in Scheme 6. We can observe that, in these structures, aluminum can be four, five or six coordinate. Moreover, in the same structures we can have more than one type of coordination. The $^{27}$Al-NMR spectrum for the tetrameric structure of aluminum isopropoxide is reported in literature by Akitt and Duncan [23] and Poncelet et al. [24]. The spectrum shows a very sharp peak of unitary intensity centered at about 0 ppm which has been attributed to the central octahedral aluminum, as well as a broad peak of triple intensity with a maximum centered at about 60–80 ppm which corresponds to the three atoms of four-coordinate aluminum in the tetramer molecule. Kriz et al. [25] give a more exact evaluation of the chemical shifts for octahedral aluminum at 3.2 and 58.5 ppm. The same authors give $^{27}$Al-NMR spectra for 9 different aluminum alkoxides confirming narrow peaks and low chemical shifts (3–5 ppm) for six-coordinate aluminum, and broader peaks and higher chemical shifts for five-coordinate (29–44 ppm) and four-coordinate (about 35–66 ppm) aluminum. Akitt [22] reports the $^{27}$Al-NMR spectra for three different aluminum alkoxides containing, respectively, the dimeric structure of

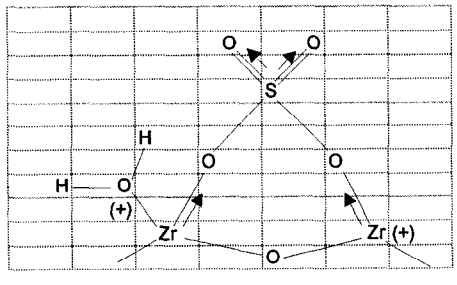


(8)

Scheme 4.

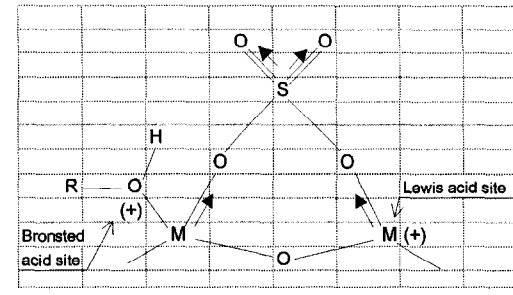


(9)

Scheme 5.

$Al(OtBu)_3$, the trimeric linear structure containing few tetramer of $Al(OiPr)_3$ and a mixture of tetramers containing also a linear tetramer with five-coordinate aluminum. According to these spectra chemical shifts for hexa-coordinate aluminum is about 3–5 ppm, for the penta-coordinate 35 ppm and for the tetra 55–65 ppm. The existence of five-coordinate aluminum has been confirmed by many authors [26–28]. In particular, Benn et al. [28] have isolated the compound $(C_2H_5)_2AlOCH_2CH_2OCH_3$ for which they determined by X-ray diffraction the structure shown in Scheme 7. The same compound examined by $^{27}$Al-NMR confirms the presence of five-coordinate aluminum. When the group $OCH_2CH_2OCH_3$ is replaced by a group $OC_2H_5$, only four-coordinate aluminum turns out at the $^{27}$Al-NMR analysis. Therefore, the presence of an ethoxy ligand favors five-coordination aluminum.

In conclusion, three types of coordination for the metal have been observed in aluminum alkoxides by $^{27}$Al-NMR analysis: they are six-coordinate aluminum with chemical shifts of 0–5 ppm, five-coordinate aluminum with chemical shifts of 30–40 ppm and four-coordinate aluminum with chemical shifts of 55–70 ppm. To the best of our knowledge, no information is available in literature for aluminum alkoxides sulphate obtained by $^{27}$Al-NMR analysis.

The spectrum of aluminum isopropoxide (Fig. 3a) shows two peaks: the narrower one is centered at 5.2 ppm whereas a much broader peak has a maximum at 62.5 ppm. Their relative ratio is 1:3 and the two resonances can be assigned to a six and a four-coordinate aluminum, respectively. The commercial product, therefore, seems to be a non linear tetramer similar to that depicted in Scheme 6.

In the spectrum of aluminum tridodecanoxide (Fig. 3b) the narrow peak at 5.2 ppm has completely disappeared, while a very broad peak centered at 63 ppm and a shoulder at about 40 ppm appear. Then, we suggest that the bulky dodecanoxide groups produce the prevalence of linear tetrameric forms with a smaller amount of pentacoordination at aluminum atoms.

The addition of sulfuric acid produces a small shift of the main broad peak from 63 to 59 and the appearance of a narrower resonance at about 3 ppm (Fig. 3c, d, e). The intensity of this peak increases with the amount of sulfuric acid and

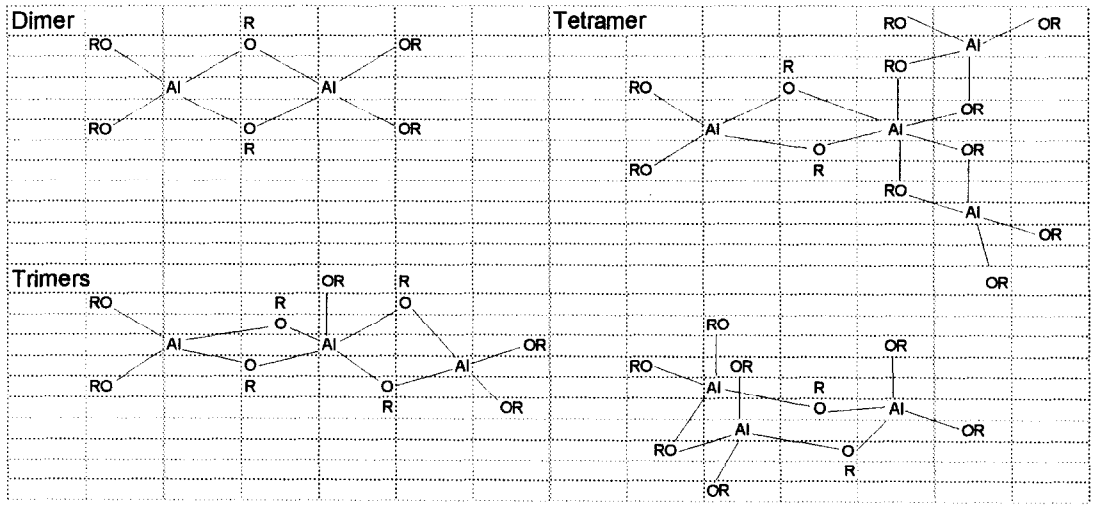


(10)

Scheme 6.

in the meantime the relative intensity of the broad resonance centered at 59 ppm decreases. When the $H_2SO_4$/Al ratio becomes 1 (Fig. 3e), two narrow peaks appear at 1.3 and −4.4 ppm, respectively. It is reasonable to conclude that sulfuric acid strongly favors the formation of the six-coordinate aluminum atoms in respect to four-coordinate ones. However, we cannot exclude the presence of five-coordinated aluminum, too. The presence of two narrow peaks at low chemical shifts can be interpreted as the existence of two types of six-coordinate aluminum different because of their near environment. By concluding, the exchange of isopropoxide with dodecanoxide groups produces local disorder, as expected. The introduction of sulfuric acid, on the contrary, increases aluminum coordination and restores local symmetry around the aluminum atom. The increase in aluminum coordination seems to be related to the catalytic activity, but we cannot completely rule out the role of the pentacoordination in the catalytic process.

### *3.3. Kinetic runs and relations between activity and catalyst acidity*

Preliminary runs have been performed in order to define the best catalyst. For comparison purposes Fig. 4 reports the kinetic behaviors of KOH, aluminum dodecanoxide and sulphated aluminum dodecanoxide with a molar ratio sulfuric acid/aluminum equal to 1. As it can be seen, the presence of sulfuric acid strongly increases the activity of the catalyst. The initial activity of the aluminum sulphated catalyst is higher than that of the classic catalyst KOH. However, this activity quickly decreases. As a consequence, the oligomers distribution is narrower as it can be appreciated in Fig. 5. Runs performed with catalysts containing different amounts of sulfuric acids show that initial activities are roughly proportional to the amount of sulfuric acid introduced, as can be seen in Fig. 6. The addition of the Lewis' base triphenylphosphine to the catalyst strongly depresses said activity, as can be seen in Fig. 7. In this

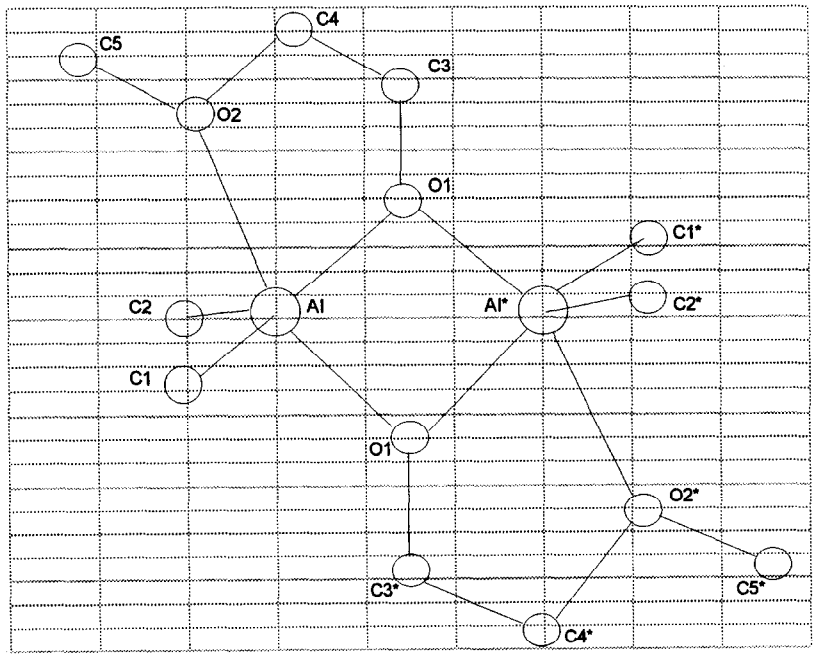


(11)

Scheme 7.

figure two runs, performed in the same operative conditions and in the presence of the same amount of catalyst (1.5% by mole of Al with ratio $Al/H_2SO_4 = 1$) one characterized by the absence of the phosphine and the other by the presence of an amount of phosphine that initially was in equimolecular concentration with respect to the catalyst, are compared. As can be seen, the phosphine strongly depresses the reaction activity by reacting with the Lewis' acid sites that are present on the aluminum catalyst. Further additions of catalyst have poor effects on the activity with a feeble increase of the reaction rates that are not comparable with the activities of unpoisoned catalyst, as can be seen in the same figure. From experimental evidence, we can conclude that the catalyst acts through the Lewis' acidity and sulfuric acid strongly enhances this type of acidity.

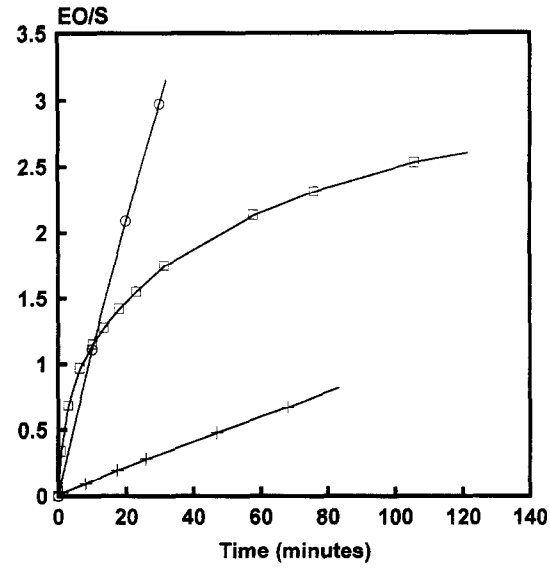


Fig. 4. Ethoxylation rate of 1-dodecanol in the presence of, respectively, KOH (○), aluminum isopropoxide (+), and aluminum isopropoxide treated with sulfuric acid in molar ratio 1:1 (□).

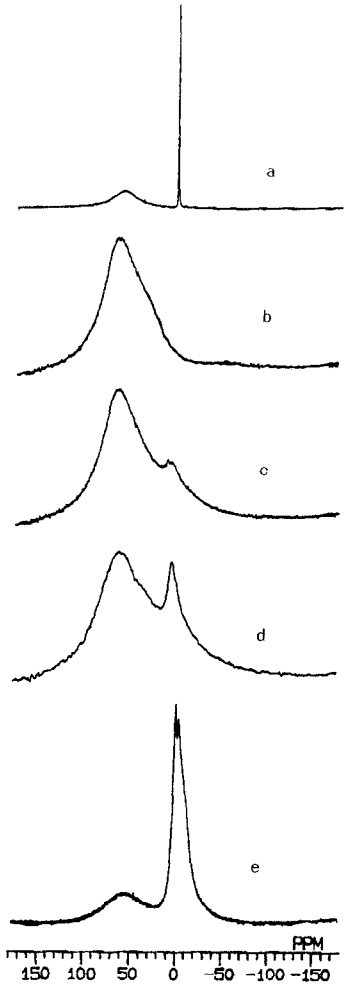


Fig. 3. $^{27}Al$ NMR spectrum obtained for aluminum isopropoxide (a), aluminum tridodecanoxide (b), and aluminum tridodecanoxide treated with sulfuric acid in molar ratio $H_2SO_4/Al = 0.25$ (c), $H_2SO_4/Al = 0.50$ (d), and $H_2SO_4/Al = 1$ (e).

Then, kinetic runs have been performed by changing temperature, pressure and catalyst concentration. Table 3 summarizes all the kinetic runs performed.

Together with dodecanol ethoxylated oligomers, small amounts of polyglycols are formed in the reaction. It is interesting to observe that the formation of polyglycols for a molar ratio of reacted ethylene oxide/substrate lower than 1 is negligible, then polyglycols are formed with a distribution being similar, as to the number of adducts, to that of ethoxylated dodecanol oligomers.

This fact suggests that polyglycols are formed by decomposition of the ethoxylated chains. Polyglycols chains can then grow independently by reacting with ethylene oxide. The formation of polyglycols should occur through the forma-

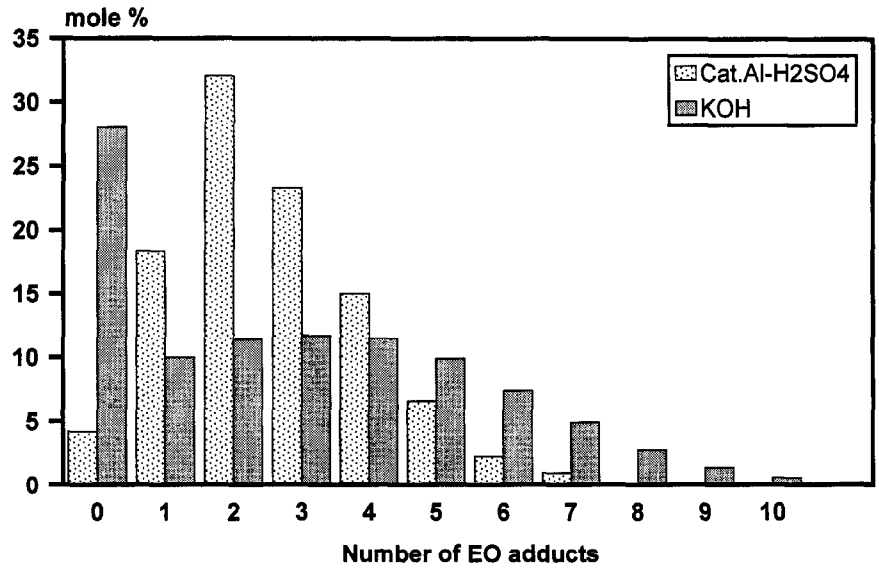


Fig. 5. Oligomers distribution obtained in the ethoxylation of 1-dodecanol in the presence of KOH and aluminum isopropoxide treated with sulfuric acid in the molar ratio 1:1, for the same ratio EO reacted/initial ROH.

tion of a carbocation and a termination with a C–C double bond. We evaluated the total amount of double bonds in the reaction mixture through the determination of the iodine number [29] and we found that the molar percentage of double bonds is almost equivalent to that of formed polyglycols.

In Table 4 the amount of polyglycols, formed at different reaction times, for each kinetic run

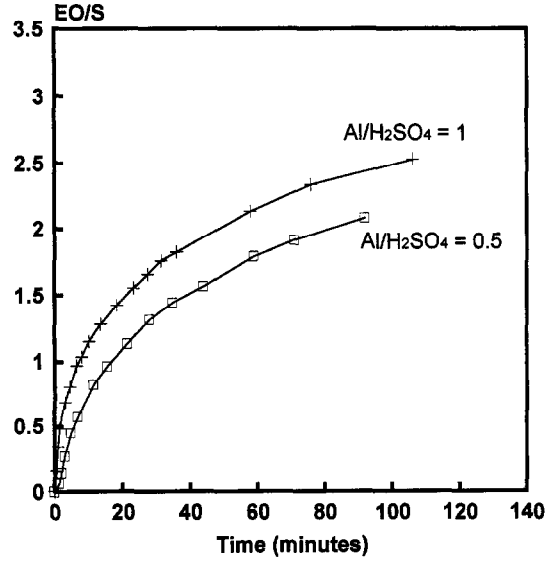


Fig. 6. Ethoxylation rate of 1-dodecanol in the presence of aluminum isopropoxide treated with sulfuric acid in the molar ratio 1:1 and 1:0.5, respectively.

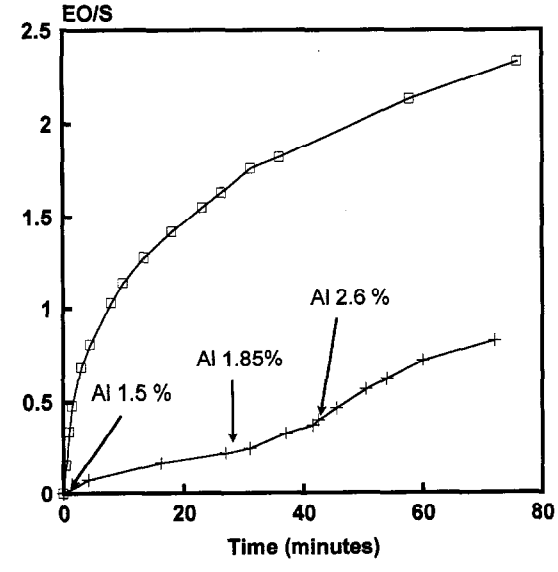


Fig. 7. Effect of the triphenylphosphine addition to the aluminum/sulfuric acid catalyst on the ethoxylation rate, at 150°C and 2 atm. Triphenylphosphine was added in a molar ratio with aluminum equal to 1. Aluminum was initially 1.5% by moles in both cases.

Table 3
List of the kinetic runs performed and related operative conditions

| Run | $P$ (atm) | $T$ (°C) | Cat. Al–$H_2SO_4$ (mol%) | $H_2SO_4$/ Al | ROH (mol) |
|---|---|---|---|---|---|
| 1 | 2 | 150 | 1.5 | 1 | 1.395 |
| 2 | 2 | 120 | 1.5 | 1 | 1.357 |
| 3 | 2 | 100 | 1.5 | 1 | 1.354 |
| 4 | 1 | 150 | 1.5 | 1 | 1.473 |
| 5 | 2 | 150 | 1.0 | 1 | 1.312 |
| 6 | 2 | 150 | 0.6 | 1 | 1.338 |
| 7 | 2 | 150 | 1.5 | 0.6 | 1.860 |

of Table 3, are reported. As can be seen, the formation of polyglycols, at the same EO/S ratio is favored by: the high temperature, the high $H_2SO_4$/Al ratio and the low pressures, respectively. These observations are in agreement with the suggested mechanism according to which the formation of polyglycols occurs via chain decomposition. However, the amounts of polyglycols formed in the seven runs of Table 4 are relatively small. Therefore, this reaction has been neglected in the successive ethoxylation kinetic analysis.

The effect of temperature on the catalyst activity can be appreciated in Fig. 8, the effect of pressure in Fig. 9 and the effect of the catalyst concentration in Fig. 10. As to oligomers distribution, it is interesting to observe that it is not affected from temperature, pressure and catalyst concentration, but only from the molar ratio (reacted ethylene oxide)/substrate. In Fig. 11, we report the evolution with the ratio (reacted ethylene oxide/substrate) of the oligomers distribution for all the runs reported in Table 3. By observing the evolution with time of the

Table 4
Amounts of polyglycols formed during the time in the kinetic runs of Table 3

| Run | Time (min) | EO/S | Total glycols (mol%) |
|---|---|---|---|
| 1 | 24 | 1.35 | 1.9 |
| | 36 | 1.67 | 2.9 |
| | 76 | 1.94 | 3.9 |
| | 106 | 2.48 | 6.7 |
| 2 | 84 | 1.83 | 1.8 |
| 3 | 140 | 1.39 | 1.3 |
| 4 | 70 | 1.36 | 2.9 |
| 5 | 27 | 0.86 | 0.8 |
| | 124 | 1.43 | 4.5 |
| 6 | 49 | 0.76 | 1.5 |
| | 127 | 1.05 | 3.8 |
| 7 | 92 | 2.03 | 2.5 |

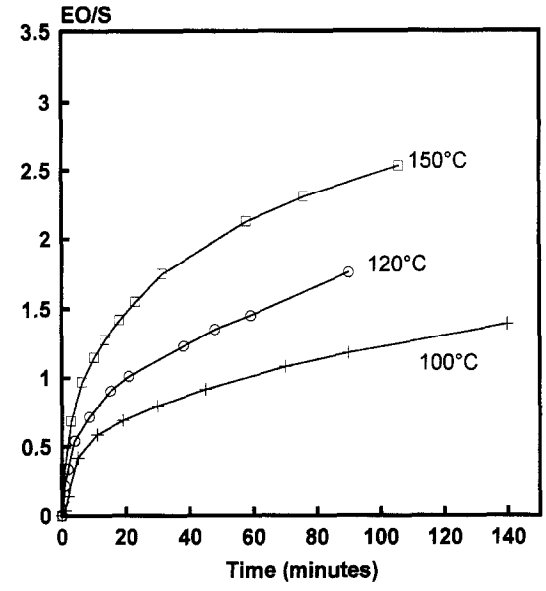


Fig. 8. Kinetic behavior of 1-dodecanol in ethoxylation performed at different temperatures.

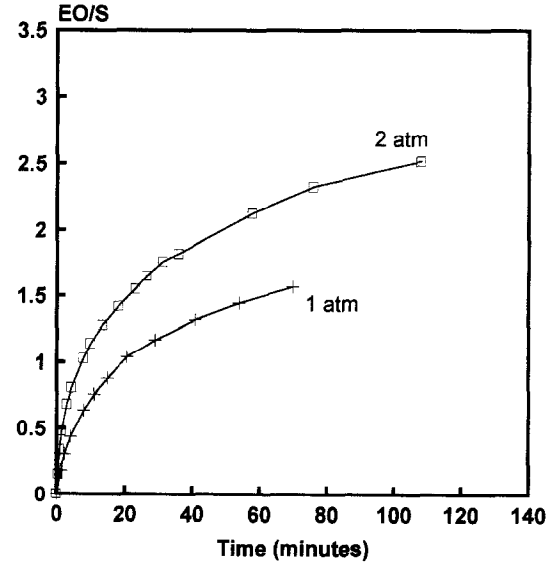


Fig. 9. Kinetic behavior of 1-dodecanol in ethoxylation performed at different pressures.

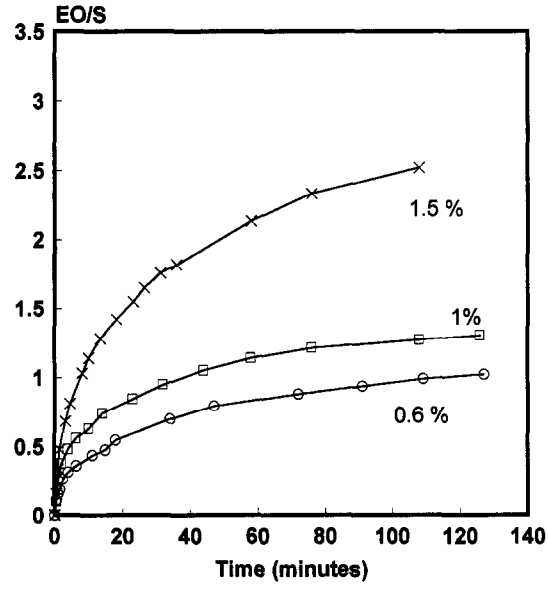


Fig. 10. Kinetic behavior of 1-dodecanol in ethoxylation performed at different catalyst concentrations.

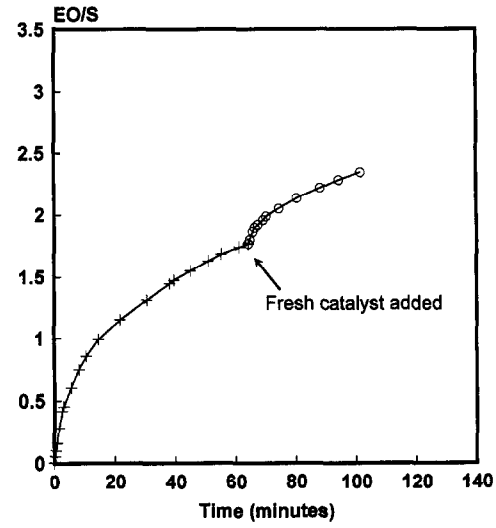


Fig. 12. Kinetic behavior in the ethoxylation of 1-dodecanol obtained by adding new fresh catalyst during the reaction. The run was performed at 120°C.

catalyst activity a question arises. Is the catalyst deactivation observed a consequence of the catalyst modification along time or a consequence of the modification of the reaction environment? In order to answer this question, we carried out a kinetic run in which fresh catalyst (50% of the initial amount) was added during the reaction.

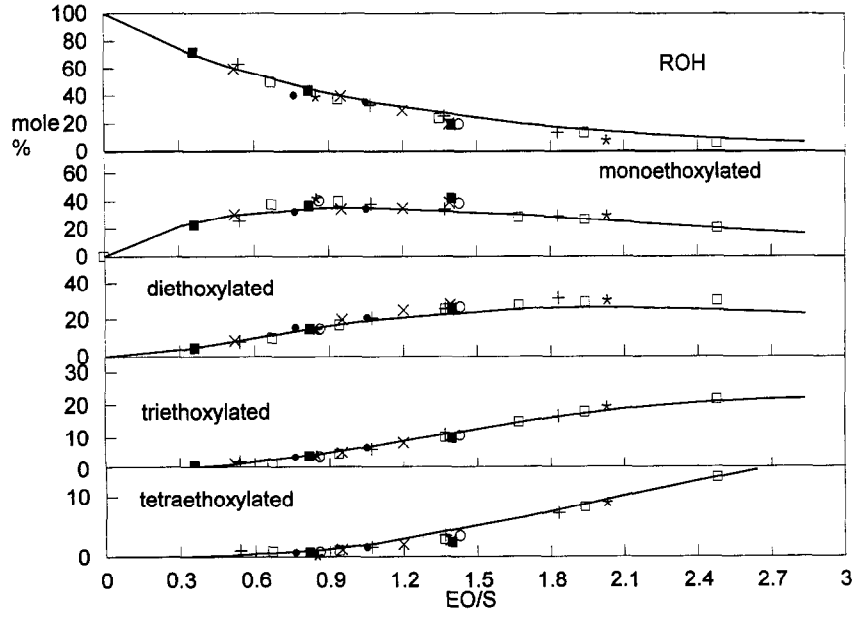


Fig. 11. The evolution with EO/S of the oligomers distribution for all the runs of Table 3. In the same figure are reported both experimental data (dots) and simulation (line) for comparison purpose. Symbols are related to: (□) run 1, (+) run 2, (×) run 3, (○) run 4, (●) run 5, (*) run 6, (■) run 7.

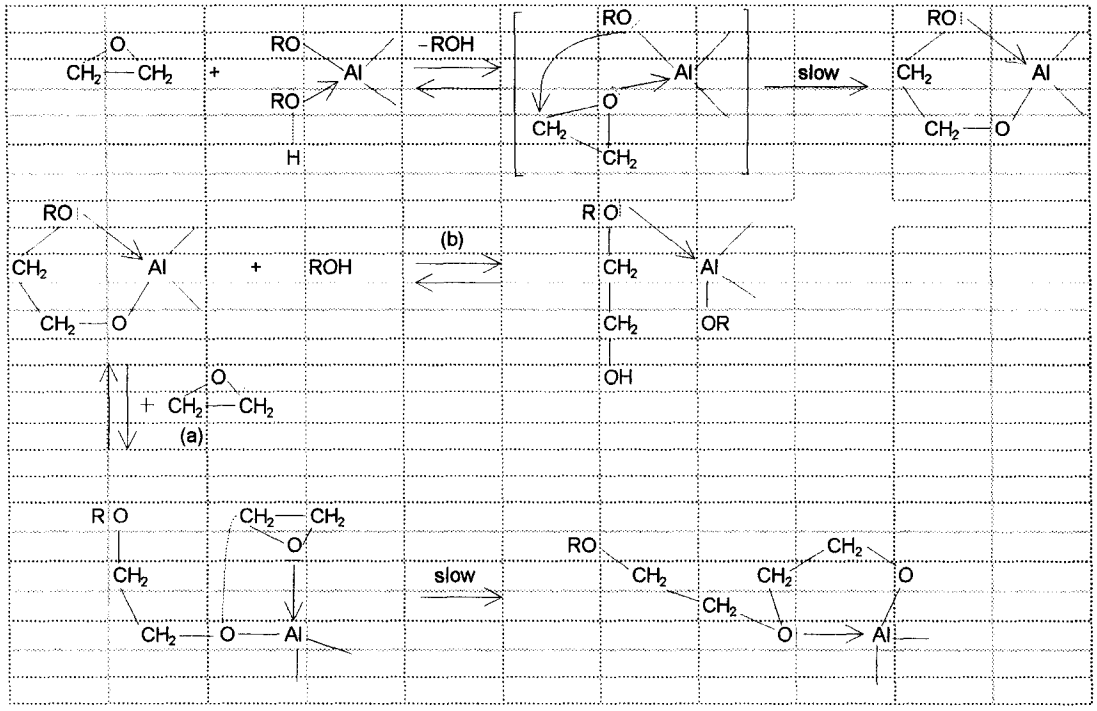


(12)

Scheme 8.

The results obtained are reported in Fig. 12. As can be seen, after a small initial increase the activity remains quite low in accordance with a depressing effect of the reaction environment. The conclusion is that ethoxylated chains have a detrimental effect on the catalytic activity.

### 3.4. Reaction mechanism and kinetic model

On the basis of the experimental observation the mechanism shown in Scheme 8 can be suggested. Ethylene oxide initially competes with dodecanol in coordinating the aluminum

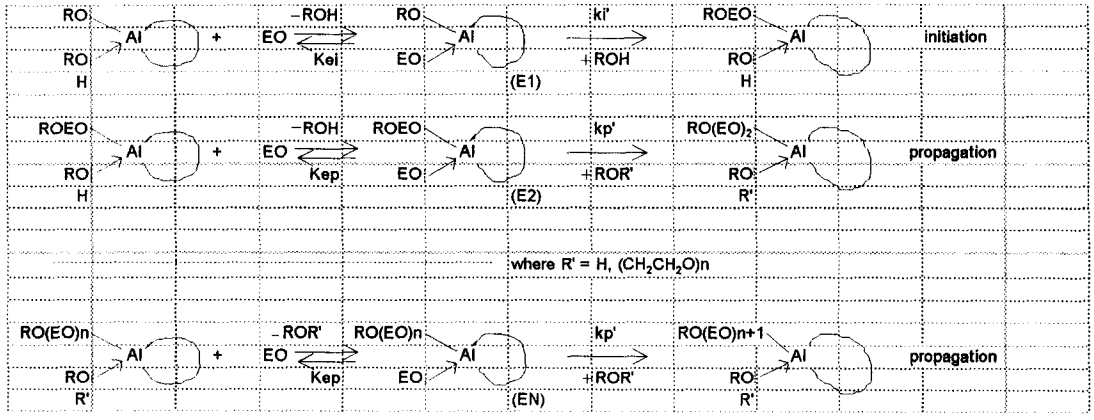


(13-15)

Scheme 9.

electron vacancy, then coordinated ethylene oxide reacts with an alkoxide bounded with aluminum. The chain can grow further (reaction (a)) or exchange the proton with a free hydroxyl group (reaction (b)). While the first equilibrium expressing the competition of ethylene oxide with alcohol is completely shifted to the right, the second one between two ethereal oxygens of ethylene oxide or ethylene oxide adduct, respectively, is probably almost equivalent in the two directions.

However, as the slow steps are successive to these mentioned equilibria, the effective kinetic constants are affected by the corresponding equilibrium constants. Therefore, we can write a simplified reaction scheme as shown in Scheme 9. Then, the proton transfer reactions must be considered, too, see Scheme 10. Proton transfer equilibrium constants, as a first approximation, must be considered independent from the chain length. The reactivity for, respectively, the initiation and any propagation step becomes, therefore:

$$r_i = k_i[E_1] = k_i' K_{ei}[RO\text{–}Al][EO] = k_i[RO\text{–}Al][EO] \quad (5)$$

$$r_p = k_p[E_N] = k_p' K_{ep}[RO(EO)_n\text{–}Al][EO] = k_p[RO(EO)_n\text{–}Al][EO] \quad (6)$$

that is, the propagation constant has been considered independent from the chain length. This assumption seems to be justified by the observation of the existence of only two kinetic regimes, one dominated by the initiation rate and the other dominated by the propagation rate. This means that the inhibitory effect of the ethoxylated chains starts at once after the formation of the first adduct. Equilibria of the type:

$$RO(EO)_n\text{–}Al + RO(EO)_mH \Leftrightarrow RO(EO)_m\text{–}Al + RO(EO)_nH \quad (7)$$

can be neglected because they can be considered as linear combinations of the reaction in Scheme 10. The previous reaction scheme can be simplified indicating with $Al_n$ the aluminum coordinated with ethoxylated dodecanol containing $n$ ethylene oxide units. Therefore:

$$Al_0 + EO \xrightarrow{k_i} Al_1 \quad (8)$$

$$Al_1 + EO \xrightarrow{k_p} Al_2 \quad (9)$$

$$\vdots$$

$$Al_n + EO \xrightarrow{k_p} Al_{n+1} \quad n = 1, 2, 3, \ldots \quad (10)$$

$$Al_n + ROH \Leftrightarrow Al_0 + RO(EO)_nH \quad n = 1, 2, 3, \ldots \quad (11)$$

On the basis of this simplified reaction scheme, we can write the following kinetic model:

$$d[n_0]/dt = -k_i[Al_0][EO] \quad (12)$$

$$d[n_1]/dt = (k_i[Al_0] - k_p[Al_1])[EO] \quad (13)$$

$$\vdots$$

$$d[n_n]/dt = k_p([Al_{n-1}] - [Al_n])[EO] \quad (14)$$

The overall mass balance on the mole of dodecanol can be assumed:

$$[RO(EO)_nH]_{TOT} = [RO(EO)_nH] + [Al_n] \approx [RO(EO)_nH] \quad (15)$$

because the concentration of the catalyst is about 1% by mole, such value being negligible in

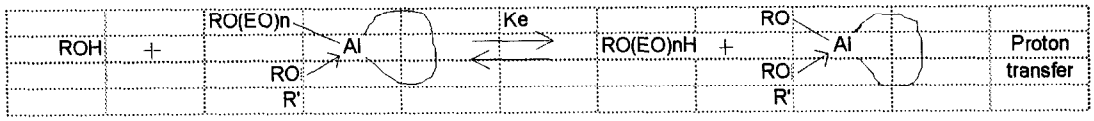


(16)

Scheme 10.

respect to the mole of dodecanol. The proton transfer equilibrium can be written as:

$$K_e = [RO(EO)_nH][Al_0]/[ROH][Al_n] \quad n = 0, 1, 2, 3, \ldots \tag{16}$$

and the aluminum mass balance will be:

$$[Al]_{TOT} = [Al_0] + [Al_1] + \ldots = \sum_i [Al_i] \tag{17}$$

From this relation, it is possible to evaluate $[Al_0]$ reminding that:

$$[Al]_{TOT} = [Al_0] \times \left\{1 + \sum_i [RO(EO)_iH]/(K_e[ROH])\right\} \tag{18}$$

hence:

$$[Al_0] = [Al]_{TOT} / \left\{1 + \sum_i [RO(EO)_iH]/(K_e[ROH])\right\} \tag{19}$$

By introducing $[Al_0]$ in Eq. (16) it is possible to find all the $[Al_n]$ values that must be used to solve the differential Eqs. (12)–(14) to determine the evolution with the time of the oligomers distribution. The evolution of the activity with time can be followed by solving the following differential equation together with the previous ones (12)–(14):

$$dnEO/dt = [EO][Al]_{TOT} \times \left\{k_i/\left(1 + \sum_i [RO(EO)_iH]/K_e[ROH]\right) + k_p \sum_i [RO(EO)_iH] / \left(K_e[ROH] + \sum_i [RO(EO)_iH]\right)\right\} V_L \tag{20}$$

Kinetic parameters of the model have been determined by mathematical regression analysis on the experimental runs 1, 2, 3 performed at

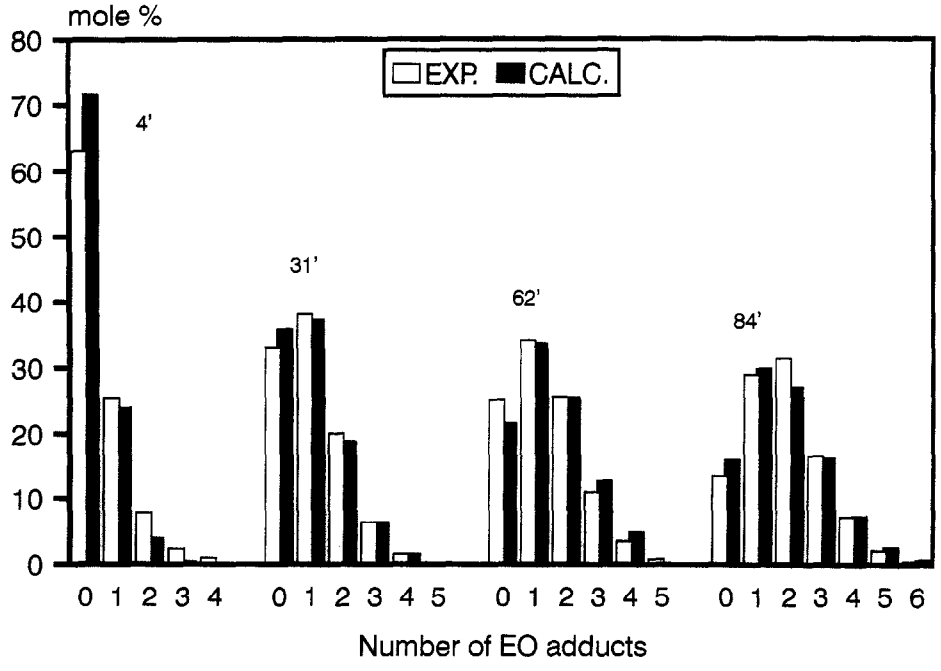


Fig. 13. An example of the evolution with time of oligomers distribution. The same figure reports both the experimental and simulated data of run 2 of Table 3 for comparison purposes.

different temperatures. Apparent kinetic parameters, obtained by the regression analysis are:

$$k_i = (1.58 \pm 0.08) \cdot 10^7 \exp[(-7760 \pm 450)/RT] \quad (21)$$

$$k_p = (3.01 \pm 0.15) \cdot 10^5 \exp[(-8400 \pm 540)/RT] \quad (22)$$

The apparent kinetic constants clearly show that initiation is largely faster than propagation mainly for the pre-exponential factor, by about 50 times. Activation energies are quite similar.

The proton transfer equilibrium constant resulted $1.3 \times 10^{-2}$ independently from temperature. This fact, together with the small difference in activation energies for respectively the initiation and the propagation is responsible for the invariance of the oligomer distributions with the operative conditions observed in Fig. 13. The low value for the proton transfer equilibrium constant confirms that aluminum complexes containing ethoxylated chains are more stable than the ones formed with dodecanol, as a consequence of the ethereal groups interaction with the electronic vacancy of the aluminum atoms.

The fitting obtained with the described kinetic model and with the kinetic parameters previously reported can be appreciated in Fig. 11 for what concerns the evolution of the oligomers distribution with the EO/S ratio and in Fig. 13, reported as an example, for the evolution of the oligomer distribution during the time for the run 2 of Table 3.

## 4. Conclusions

Reacting sulfuric acid with aluminum tridodecanoxide gives place to catalysts that are characterized by a very strong Lewis acidity and are completely soluble in hydrophobic solvents such as dodecanol.

The ethoxylation of dodecanol is strongly promoted by this kind of catalysts, especially for the reaction with the first adduct.

The addition of two or more ethylene oxide groups occurs much slowly. A narrow range distribution of the oligomers is, therefore, obtained as a consequence of this particular behavior of the catalyst.

The reason of this behavior is that initially ethylene oxide easily shift dodecanol coordinated to aluminum and reacts with a dodecanoxide group bounded to aluminum. When ethoxylated dodecanol accumulates in the reaction mixture, competition occurs between ethylene oxide molecules and the ethereal oxygen of the ethoxylated chains for the interaction with the aluminum electronic vacancy. The effect is a drastic change in the kinetic regime and the obtainment of a narrow distribution.

The active sites seem to be hexa-coordinated aluminum, however the possibility of the intervention of the penta-coordinated one cannot be excluded.

## 5. Nomenclature

| | |
|---|---|
| $[Al_0], [Al_1], \ldots, [Al_n] =$ | Concentration of aluminum complexes containing respectively the groups RO–, RO(EO)–, RO(EO)$_n$– (mol/cm$^3$). |
| $[Al_{TOT}]$ | = Total concentration of the aluminum catalyst (mol/cm$^3$). |
| [EO] | = Concentration of ethylene oxide in liquid phase (mol/cm$^3$). |
| $K_e$ | = Equilibrium constant for proton transfer reactions. |
| $K_{ei}$ | = Equilibrium constant of the reaction preceding the reaction of initiation. |
| $K_{ep}$ | = Equilibrium constant of the reaction preceding the reaction of propagation. |

$k_i$ = Initiation reaction apparent kinetic constant ($cm^3/mol\ s$).

$k_p$ = Propagation reaction apparent kinetic constant ($cm^3/mol\ s$).

$[n_i]$ = Concentration of the oligomer with $i$ adducts ($mol/cm^3$).

$n_{EO}$ = Number of ethylene oxide moles consumed per mole of substrate.

$r_i$, $r_p$ = Reaction rates of respectively initiation and propagation ($mol/cm^3\ s$).

$[RO(EO)_iOH]$ = Concentration of the oligomer containing $i$ adducts ($mol/cm^3$).

## Acknowledgements

Thanks are due to Pressindustria Spa and Consiglio Nazionale delle Ricerche, Progetto Finalizzato Chimica Fine II for financial support.

## References

[1] K.L. Matheson and P.A. Schwab, Proc. of the 3rd CESIO Int. Surfactants World Congr. and Exhibition (London, 1991) p. 291.
[2] E. Santacesaria, M. Di Serio and L. Lisi, Ind. Eng. Chem. Res. 29 (1990) 719.
[3] E. Santacesaria, M. Di Serio, R. Garaffa and G. Addino, Ind. Eng. Chem. Res. 31 (1992) 2413.
[4] M. Di Serio, S. Di Martino and E. Santacesaria, Ind. Eng. Chem. Res. 3 (1994) 509, 514.
[5] M. Di Serio, R. Tesser, F. Felippone and E. Santacesaria, Ind. Eng. Chem. Res. (1995), in press.
[6] E. Santacesaria, M. Di Serio, R. Garaffa and G. Addino, Ind. Eng. Chem. Res. 31 (1992) 2419.
[7] G.L. Nield, P.H. Washecheck and K. Yang, U.S. Patent 4,210,764 (1980).
[8] K. Yang, G.L. Nield and P.H. Washecheck, U.S. Patent 4,223,164 (1980).
[9] European Patent 104,309 (1984).
[10] C.L. Edwards, U.S. Patent 4,721,816 (1988).
[11] C.L. Edwards, U.S. Patent 4,721,817 (1988).
[12] N.A. Benesi, J. Phys. Chem. 61 (1957) 970.
[13] P.L. Desberre, B. Desmaziares, V. Even, J.J. Bosselier and L. Minssieux, Chromatographia 24 (1987).
[14] K. Nakanishi, Infrared Absorption Spectroscopy (Holden-Day, San Francisco, 1962) p. 20.
[15] C.G. Barraclough, D.C. Bradley, J. Lewis and I.M. Thomas, J. Chem. Soc. (1961) 2601.
[16] K. Nakamoto, Infrared Spectra of Inorganic and Coordination Compounds (Wiley Interscience, New York, 1970) pp. 173–175, and references therein.
[17] J.R. Ferraro and A. Walken, J. Chem. Phys. 42 (1965) 1278.
[18] M. Hino and K. Arata, Hyomen 19 (1981) 75.
[19] K. Arata, Advances in Catalysis, Vol. 37 (1990) p. 165.
[20] M. Misono and T. Okuhara, CHEMTECH November (1993) 23.
[21] P.W.N.M. Van Leeuwen, Rec. Trav. Chim. Pays-Bas 86 (1967) 247.
[22] J.W. Akitt, Progress in NMR Spectroscopy, Vol. 21 (1989) pp. 1–149.
[23] J.W. Akitt and R.H. Duncan, J. Magn. Reson. 15 (1974) 162.
[24] K. Folting, W.E. Streib, K.G. Carlton, O. Poncelet and L.G. Hubert-Pfalzgral, Polyhedron 10 (1991) 1639.
[25] O. Kriz, B. Casensky, A. Lyca, J. Fusek and S. Hermanek, J. Magn. Reson. 60 (1984) 375.
[26] D.A. Stephenson and P.B. Moore, Acta Crystallogr., Sect. B 24 (1968) 1518.
[27] M.C. Cruickshank, L.S. Dent Glasser, Sami A.I. Barri and Ian J.F. Poplett, J. Chem. Soc., Chem. Commun. P 23 (1986).
[28] R. Benn, A. Rufinska, H. Lehmkuhl, E. Janssen and C. Kruger, Angew. Chem. Int. Ed. Engl. 22 (1983) 779.
[29] ASTM D (1959) 85.